Structural Engineering and Mechanics, Vol. 5, No. 5 (1997) 645-662
DOI: http://dx.doi.org/10.12989/sem.1997.5.5.645

Layered finite element method in cracking and failure analysis of RC beams and beam-column-slab connections

Hong Guan†

Finite Element Analysis Research Centre, Engineering Faculty, University of Sydney, NSW 2006, Australia

Yew-Chaye Loo‡

School of Engineering, Griffith University, Gold Coast Campus, QLD 4217, Australia

Abstract. A nonlinear semi-three-dimensional layered finite element procedure is developed for cracking and failure analysis of reinforced concrete beams and the spandrel beam-column-slab connections of flat plates. The layered element approach takes the elasto-plastic failure behaviour and geometric nonlinearity into consideration. A strain-hardening plasticity concrete model and a smeared steel model are incorporated into the layered element formulation. Further, shear failure, transverse reinforcement, spandrel beams and columns are successfully modelled. The proposed method incorporating the nonlinear constitutive models for concrete and steel is implemented in a finite element program. Test specimens including a series of reinforced concrete beams and beam-column-slab connections of flat plates are analysed. Results confirm the effectiveness and accuracy of the layered procedure in predicting both flexural and shear cracking up to failure.

Key words: layered finite element; crack; failure analysis; reinforced concrete; beam; beam-column-slab connection; flate plate.

1. Introduction

In the analysis of reinforced concrete structures such as flat plates, slabs and beams, predicting the transverse shear failure is one of the most formidable tasks. Three-dimensional solid elements are commonly used to analyse both flexural and shear failures. However, the disadvantage of using three-dimensional elements lies in the excessive number of unknown degrees of freedom associated with a large bandwidth. As a result, a large amount of computing time is required and the computer output is relatively complicated which necessitates special management effort.

The layered finite element method has been used to solve three-dimensional problems of reinforced concrete structures, particularly in analysing the flexural behaviour of plates and shells. Incorporating the layered approach, Owen and Figueiras (1984) and Harmon and Ni (1989) studied the transverse shear response of reinforced concrete plates and shells. However, the shear failure analysis of beam-column-slab connections in flat plates by the finite element method

† Research Fellow
‡ Professor and Head

has not been adequately studied.

A semi-three-dimensional layered model is developed by encompassing all the in-plane and out-of-plane stress components in a finite element formulation. Incorporating the nonlinear constitutive models for concrete and steel, the proposed procedure is capable of analysing both flexural and shear cracking up to failure. In addition, the spandrel beams are modelled by using the stiffness transformation technique and the transverse reinforcement is included by adding its contributions to the material matrix which corresponds to the normal strain in the transverse direction. These made possible the simulation of spandrel beams and closed ties.

2. Semi-three-dimensional layered approach

In the layered approach (Guan and Loo 1994), each element is subdivided into a chosen number of layers which are fully bonded together (see Fig. 1). The concrete characteristics are specified individually for each layer over its thickness. On the other hand, each layer of the reinforcing bars is represented by a smeared layer of equivalent thickness.

An eight-node degenerated shell element with bi-quadratic serendipity shape functions is adopted in conjunction with the layered approach. The model makes use of the transverse shear deformations associated with the Mindlin hypothesis. Five d.o.f. are specified at each nodal point. They are the in-plane displacements, u and v, transverse displacement w, and two independent bending rotations about the x and y axes, i.e., θy and θx respectively.

In a nonlinear analysis, the material state at any Gauss point located at the mid-surface of a layer, can be elastic, plastic or fractured according to the loading history. To account for the mechanical change of the materials throughout the incremental loading process, cracking and nonlinear material response are traced layer by layer.

By incorporating all the in-plane and out-of-plane stress components in the finite element formulation, the proposed layered element is capable of simulating inclined cracks. As a result,

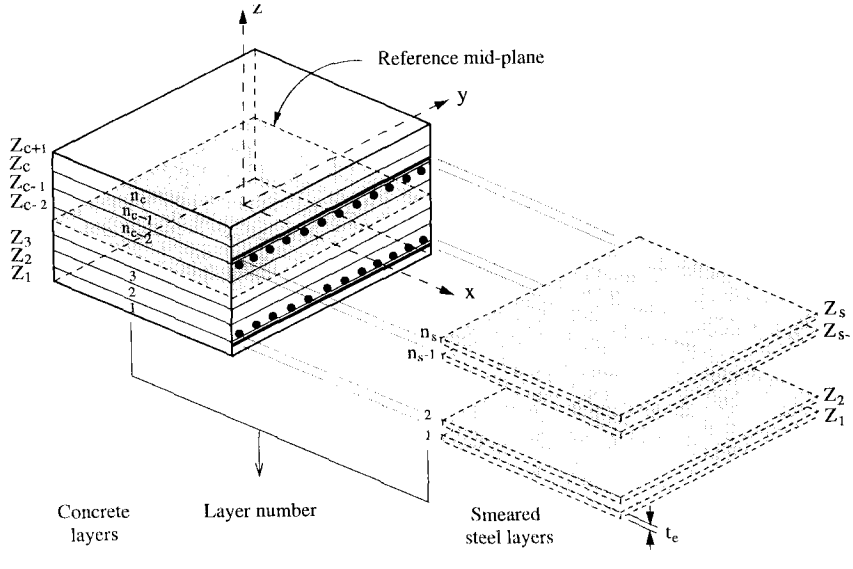

Fig. 1 Layered model.

the prediction of transverse shear failure and punching shear failure of flat plates becomes possible without resorting to the use of expensive fully three-dimensional elements.

3. Modelling of spandrel beams

Reinforced concrete flat plates usually incorporate spandrel beams or band beams to strengthen the slab-column connections and reduce the possibilities of punching shear failure. These slabs have arbitrarily and eccentrically stepped thicknesses in their geometry. The upper surface of the slab is flat and the variation of the thickness is restricted to the lower surface. Hence the location of the mid-surface varies according to the variation of the thickness. However, it can be assumed that the mid-surface of the entire slab is located at the plane that bisects the slab thickness.

Consider a flat plate stiffened by an offset spandrel beam along its edge, as shown in Fig. 2. The nodal points of the beam do not coincide with those of the slab. The boundary conditions are simulated by carrying out the coordinate transformation technique to "slave" the degrees of freedom of the beam to the "master" degrees of freedom of the slab in the assembled structure. Based on the concept of "rigid links" (Cook, *et al.* 1989), a simplified approach is developed to take into account the eccentricities of the spandrel beams and the columns in flat plates.

In general, a typical node of the beam is to be transferred to the corresponding node of the slab. This is accomplished by adding an imaginary, weightless but rigid link between nodes i_{beam} and i_{slab}. Assuming that the spandrel beams are also built up of layered elements, the coordinate transformation can be achieved as follows

$$\begin{Bmatrix} u_i \\ v_i \\ w_i \\ \theta_{xi} \\ \theta_{yi} \end{Bmatrix}_{beam} = \begin{bmatrix} 1 & 0 & 0 & d_o & 0 \\ 0 & 1 & 0 & 0 & -d_o \\ 0 & 0 & 1 & 0 & 0 \\ 0 & 0 & 0 & 1 & 0 \\ 0 & 0 & 0 & 0 & 1 \end{bmatrix} \begin{Bmatrix} u_i \\ v_i \\ w_i \\ \theta_{xi} \\ \theta_{yi} \end{Bmatrix}_{slab} \tag{1}$$

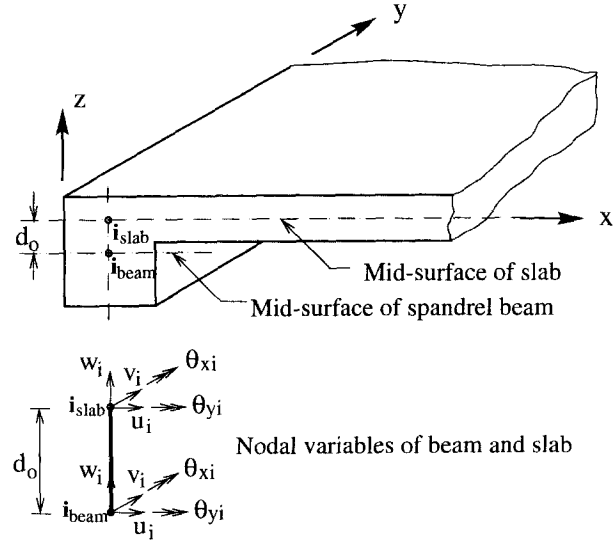

Fig. 2 Description of nodal variables of spandrel beam and adjoining slab.

or
$$\{U\}_{beam}=[T_o]\ \{U\}_{slab} \tag{2}$$

where $\{U\}_{beam}$ and $\{U\}_{slab}$ contain the nodal displacements of the offset beam element and the slab element, respectively; $[T_o]$ is the transformation matrix of the offset element; d_o is the distance between the mid-surface of the beam and that of the slab. In Eq. (1), the products $d_o\theta_{xi}$ and $-d_o\theta_{yi}$ are the displacements in x- and y- directions, respectively. This transformation procedure can be applied wherever the offset element exists.

Correspondingly the element stiffness matrix $[K_e]$ and internal force vector $\{r_e\}$, associated with a slab element, can be obtained through the transformation from $[K_o]$ and $\{r_o\}$, of the offset element. Or,

$$[K_e]=[T]^T\ [K_o]\ [T] \tag{3}$$

and
$$\{r_e\}=[T]^T\{r_o\} \tag{4}$$

where
$$[T]_{40\times 40}=\begin{bmatrix} [T_o] & & & & & & & \\ & [T_o] & & & & & & \\ & & [T_o] & & & 0 & & \\ & & & [T_o] & & & & \\ & & 0 & & [T_o] & & & \\ & & & & & [T_o] & & \\ & & & & & & [T_o] & \\ & & & & & & & [T_o] \end{bmatrix} \tag{5}$$

for an 8-node element.

The layered procedure used for simulating the slab and the beam is also applied to the monolithically cast concrete columns. As a result the columns may crack or fail should such conditions exist under load. The column supports are modelled in such a way that they are provided at their bottom surfaces, rather than at the mid-heights of the slab. Hence the real support conditions can be modelled correctly. This was achieved by doubling the distance d_o between the mid-surface of the slab and bottom surface of the column.

4. Analytical model

In the proposed analysis, the failure of reinforced concrete is considered to be a result of either tension cracking in concrete or plastic yielding which leads to the crushing of concrete (Guan and Loo 1996).

Concrete is assumed to be linear elastic and its behaviour is characterised as isotropic until the specified fracture surface is reached. The constitutive equation for isotropic material, in the material coordinate system ($x'y'z'$), can be expressed as

$$d\{\sigma\}=[\bar{D}_c]d\{\varepsilon\} \tag{6}$$

where
$$[\bar{\boldsymbol{D}}_c]=\begin{bmatrix} K+\frac{4}{3}G & K-\frac{2}{3}G & K-\frac{2}{3}G & 0 & 0 & 0 \\ & K+\frac{4}{3}G & K-\frac{2}{3}G & 0 & 0 & 0 \\ & & K+\frac{4}{3}G & 0 & 0 & 0 \\ & & & G & 0 & 0 \\ & & & & G & 0 \\ & & & & & G \end{bmatrix} \tag{7}$$

in which K and G are the bulk and shear moduli, respectively.

The tension cut-off representation is adopted to model the concrete in tension in which cracking is governed by the maximum tensile stress criterion. Cracked concrete is treated as an orthotropic material using a smeared crack approach. After cracking has occurred, the tensile and shear stresses acting on the crack plane are released and redistributed to the neighbouring elements. Under subsequent loading, concrete loses its tensile strength normal to the crack direction, but retains the tensile strength in the directions parallel to the crack plane. The constitutive equation for cracked concrete is given as

$$d\{\sigma\}=[\boldsymbol{D}_{cr}]d\{\varepsilon\} \tag{8}$$

where
$$[\boldsymbol{D}_{cr}]=\begin{bmatrix} E_i & 0 & 0 & 0 & 0 & 0 \\ & E_2 & \frac{\nu\sqrt{E_2E_3}}{1-\nu-2\nu^2} & 0 & 0 & 0 \\ & & E_3 & 0 & 0 & 0 \\ & & & G_{12}^c & 0 & 0 \\ & \text{Symm} & & & G_{13}^c & 0 \\ & & & & & G_{23}^c \end{bmatrix} \tag{9a}$$

or
$$[\boldsymbol{D}_{cr}]=\begin{bmatrix} E_i & 0 & 0 & 0 & 0 & 0 \\ & E_i & 0 & 0 & 0 & 0 \\ & & E_3 & 0 & 0 & 0 \\ & & & G_{12}^{c'} & 0 & 0 \\ & \text{Symm} & & & G_{13}^{c'} & 0 \\ & & & & & G_{23}^{c'} \end{bmatrix} \tag{9b}$$

for concrete cracked in one and two directions, respectively. In Eqs. (9a) and (9b), E_i is the fictitious modulus of elasticity which accounts for the tension stiffening effect; G_{12}^c, G_{13}^c, G_{23}^c and $G_{12}^{c'}$, $G_{13}^{c'}$, $G_{23}^{c'}$ are the modified cracked shear moduli (Guan 1996).

The strain-hardening plasticity approach used by Owen and Figueiras (1984) is adopted to model the concrete in compression. This approach involves loading surfaces, loading function, normality rule as well as unloading. The elasto-plastic constitutive equation is expressed as

$$d\{\sigma\}=[\boldsymbol{D}_{ep}]d\{\varepsilon\} \tag{10}$$

where
$$[\boldsymbol{D}_{ep}]=[\bar{\boldsymbol{D}}'_c]-\frac{\boldsymbol{d}_D\,\boldsymbol{d}_D^T}{H'+\boldsymbol{d}^T\boldsymbol{a}} \tag{11a}$$

and
$$\boldsymbol{d}_D=[\bar{\boldsymbol{D}}'_c]\boldsymbol{a} \tag{11b}$$

In Eqs. (11a) and (11b), $[\bar{\boldsymbol{D}}'_c]=[\boldsymbol{T}_{\varepsilon'}]^T[\bar{\boldsymbol{D}}_c][\boldsymbol{T}_{\varepsilon'}]$ if the principal axes do not coincide with the reference axes x', y' and z'; $\boldsymbol{a}$ is the flow vector and H' is the hardening parameter associated with the expansion of the yield surface. Note that $[\boldsymbol{T}_{\varepsilon'}]$ is the transformation matrix for strain components between the local and material coordinate systems.

After the compression type of fracture occurs, the concrete material is assumed to lose some, but not all, of its strength and rigidity. This requires that in Eq. (7), the bulk modulus K retains its original value and this leads to the following constitutive matrix

$$[\boldsymbol{D}_{crs}]=\begin{bmatrix} K & K & K & 0 & 0 & 0 \\ & K & K & 0 & 0 & 0 \\ & & K & 0 & 0 & 0 \\ & & & 0 & 0 & 0 \\ & \text{Symm} & & & 0 & 0 \\ & & & & & 0 \end{bmatrix} \tag{12}$$

Numerical modelling of either cracking or crushing of concrete involves the modification of material stiffness and the release of the appropriate stresses partially or completely in the fractured elements.

The reinforcing steel is assumed to be elastic-plastic uniaxial material. The reinforcing bars at a given level in an element are modelled as a smeared steel layer of equivalent thickness. For a steel layer, the constitutive equation may be given as

$$d\{\sigma\}=[\bar{\boldsymbol{D}}_s]d\{\varepsilon\} \tag{13}$$

where the material matrix in the material coordinate system

$$[\bar{\boldsymbol{D}}_s]=\begin{bmatrix} \rho_s E_s & 0 & 0 & 0 & 0 & 0 \\ & 0 & 0 & 0 & 0 & 0 \\ & & 0 & 0 & 0 & 0 \\ & & & 0 & 0 & 0 \\ & \text{Symm} & & & 0 & 0 \\ & & & & & 0 \end{bmatrix} \tag{14}$$

in which ρ_s ($s=x'$, y') is the reinforcement ratio (in the x'- and y'-directions) in the steel layer and E_s is the Young's modulus of steel.

Once concrete has cracked, the material axes coincide with the principal stress directions, therefore $[\boldsymbol{D}_{cr}]$ in Eqs. (9a) and (9b) must be transformed from the principal axes to the local xyz coordinate system. Or,

$$[\bar{\boldsymbol{D}}'_c]=[\boldsymbol{T}_{\varepsilon'}]^T[\boldsymbol{D}_{cr}][\boldsymbol{T}_{\varepsilon'}] \tag{15}$$

Similarly, if the directions of the steel bars do not coincide with the x-axis, $[\bar{\boldsymbol{D}}_s]$ in Eq. (14) must also be transformed into the local coordinate system as

$$[\bar{D}'_s]=[T_{\varepsilon'}]^T[\bar{D}_s][T_{\varepsilon'}] \tag{16}$$

The total element material constitutive matrix, containing the contributions of concrete and steel, can be calculated by direct superposition. Or,

$$[\bar{D}']=\sum_{i=1}^{n_c}[\bar{D}_c]+\sum_{i=1}^{n_s}[\bar{D}'_s] \tag{17}$$

where $[\bar{D}_c]$ can be taken as $[\bar{D}'_c]$ (Eq. (15)), $[D_{ep}]$ (Eq. (11a)) or $[D_{crs}]$ (Eq. (12)) depending on the stress condition considered; n_c and n_s respectively are the total number of concrete and steel layers (see Fig. 1).

In Eq. (17), $[\bar{D}']$ is of size 6×6. However due to the conventional plane stress assumption ($\sigma_z=0$), $[\bar{D}']$ must be condensed into $[\bar{D}]$ (of size 5×5). Or,

$$[\bar{D}(i,j)]=[\bar{D}'(i+m,j+n)]-\frac{[\bar{D}'(i+m,3)]\ [\bar{D}'(3,j+n)]}{[\bar{D}'(3,3)]} \tag{18}$$

where $m=0$, $(1\leq i\leq 2)$; $m=1$, $(3\leq i\leq 5)$; $n=0$, $(1\leq j\leq 2)$; $n=1$, $(3\leq j\leq 5)$.

In Eq. (18),

$$[\bar{D}'(3,3)]=[\bar{D}_c(3,3)]+\rho_{z'}E_s \tag{19}$$

which implies that the effect of the out-of-plane reinforcement can be included by adding its contributions to the material matrix which corresponds to the normal strain in the transverse direction.

Having the total material matrix determined for each element, the stiffness matrix for the corresponding element can be evaluated and the global stiffness matrix is then assembled using the standard procedure. An incremental and iterative procedure is used to obtain the nonlinear solution and the computer program (Guan 1996) developed in this study is capable of reproducing the nonlinear behaviour caused by both material and geometric nonliearities.

5. Numerical investigations

5.1. Simply supported beams with or without web reinforcement

The results from the series of simply supported, reinforced concrete beams tested by Bresler and Scordelis (1963) have become a benchmark for checking computer based reinforced concrete analyses. This is because the tests which included both brittle and ductile failure cases covered a wide-ranging variation in beam geometry, and tensile and web reinforcements. These test results are used herein to verify the capability of the proposed layered model in simulating transverse reinforcements.

Bresler and Scordelis's tests (1963) were to determine the cracking load and ultimate strength of a specially designed series of 12 beams. Each beam is subjected to a concentrated load applied at mid-span as illustrated in Fig. 3. The test beams were grouped into four series (Series *OA, A, B*, and *C*). The first two groups, the *OA*-series (which were without web reinforcement) and the *A*-series (with web reinforcement), are analysed herein. The dimensions of the beams and their corresponding material properties given in the original publication (Bresler and Scordelis

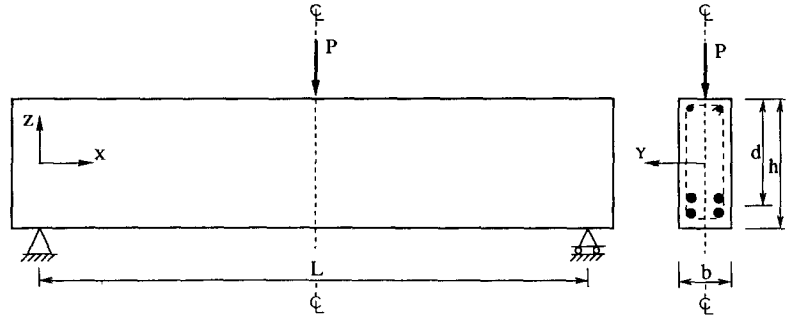

Fig. 3 Simply supported beam under central concentrated load.

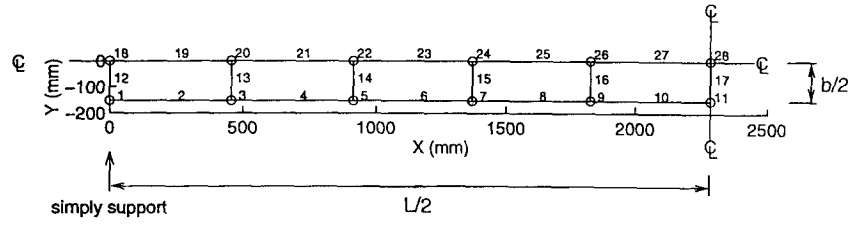

(a) Mesh

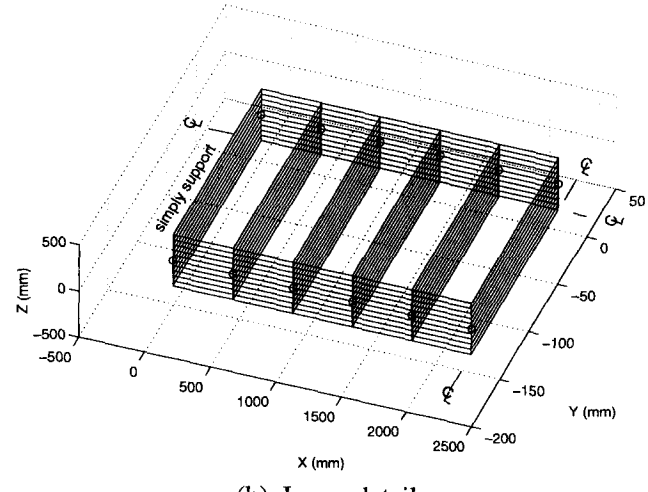

(b) Layer details

Fig. 4 Finite element idealisation of a typical beam (*OA*-2).

1963) are adopted in the present analysis. Owing to the existence of two planes of symmetry only one quarter of each beam is analysed. The finite element idealisation of a typical beam (*OA*-2) is presented in Fig. 4.

5.1.1. Beams without web reinforcement

Fig. 5 compares the predicted load-deflection curves at the mid-span section of the *OA*-series

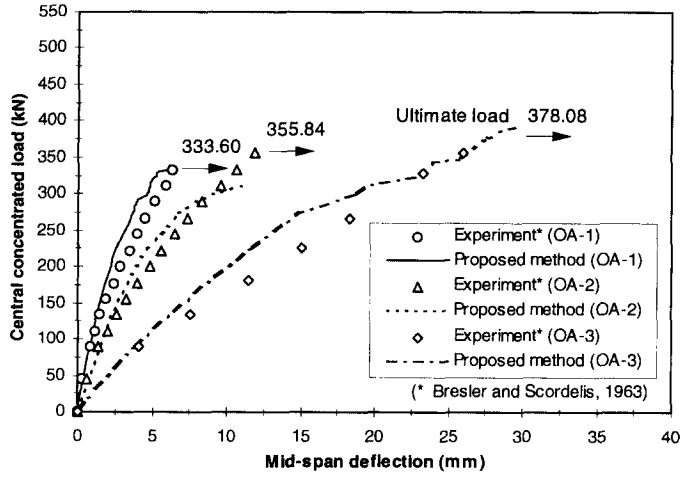

Fig. 5 Comparison of load-deflection results for *OA*-series beams.

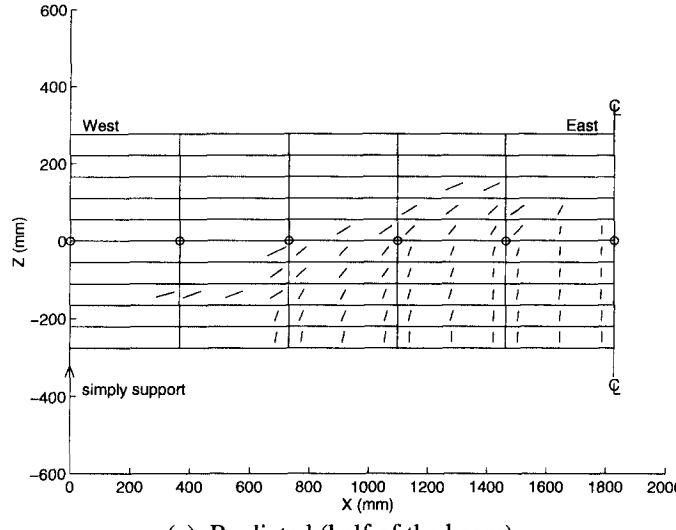

(a) Predicted (half of the beam)

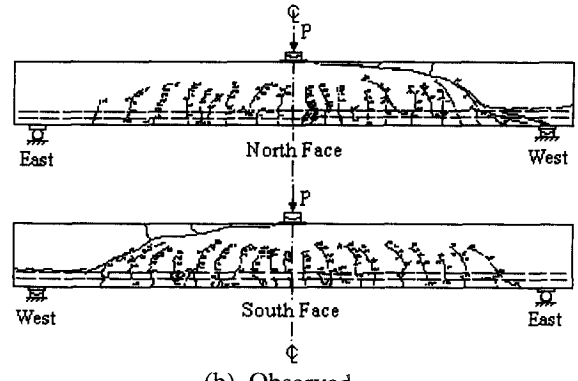

(b) Observed

Fig. 6 Crack patterns for beam *OA*-2.

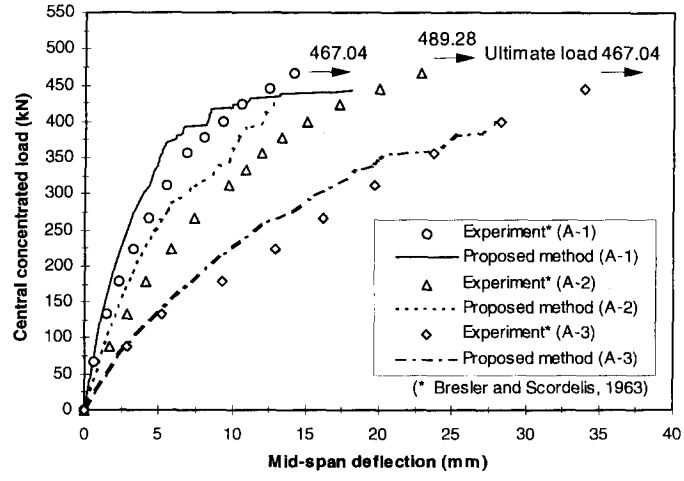

Fig. 7 Comparison of load-deflection results for *A*-series beams.

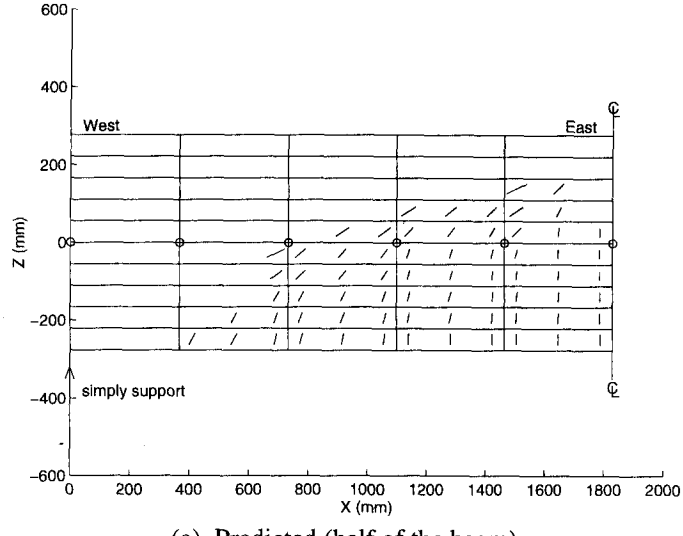

(a) Predicted (half of the beam)

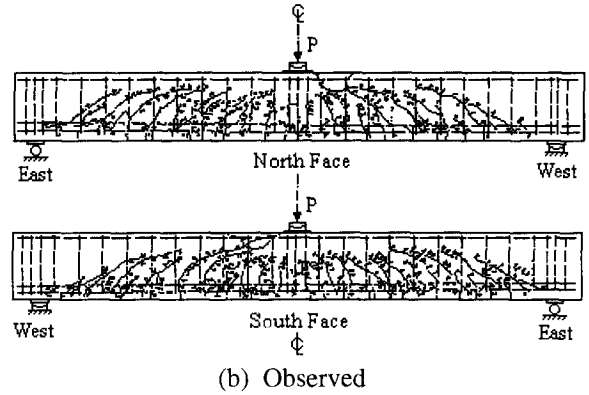

(b) Observed

Fig. 8 Crack patterns for beam *A*-2.

beams with the experimental results. Good correlations are observed. Note that the ultimate loads shown in this and subsequent load-deflection plots are the measured values. As may be seen in the figure, some horizontal steps may be seen in the load-deflection curves. They are caused by a tensile or compressive failure in one of the elements which is followed by a decrease in the structural stiffness under additional load.

In the experiment, all the beams in the *OA*-series failed in a "shear-tension" mode (Loo 1990). Fig. 6 shows the crack patterns for beam *OA*-2 which characterise this type of failure. Included in the same figure is the predicted crack patterns (for half of the beam). The agreement is reasonably good.

5.1.2. Beams with web reinforcement (closed ties)

For the *A*-series beams which were with web reinforcement, the load-deflection response compares fairly well with the experimental results, as evident in Fig. 7. It may be seen in the figure that for Beams *A*-1 and *A*-2, failures occurred immediately after the measurement of the maximum deflection. On the other hand, Beam *A*-3 sustained a much larger deformation before collapse. Correspondingly, the predicted load-deflection curve for Beam *A*-3 shows a rapid increase of deflections due to the yielding of steel. As a result, the ultimate deflections of Beam *A*-3 is much larger than that of *A*-1 and *A*-2.

The predicted and observed crack patterns for a typical beam, *A*-2, with web reinforcement, are compared in Fig. 8. Again good agreement is obtained.

5.1.3. Comparison of ultimate loads

The comparison of predicted and measured ultimate load values for all the beam series is summarised in Table 1. The analytical load-deflection curves (Figs. 5 and 7) replicate, with accepted accuracy, the experimental responses. However, the analysis leads to a slightly lower ultimate load, except for Beams *OA*-1 and *OA*-3. The ratios of the predicted and measured ultimate loads range from 0.86 to 1.04, with a mean of 0.94. This is considered a satisfactory prediction.

To demonstrate the accuracy achievable using the proposed semi-three-dimensional layered element model, a further comparison of results is carried out. For Beams *OA*-1 and *A*-1, Table 2 shows in addition to the experimental ultimate loads, the predicted values due to the proposed

Table 1 Comparison of ultimate load of simply supported beams

Beam	Failure mode	Ultimate load		
		Experiment (kN)	Proposed method (kN)	Proposed / Experiment
OA-1	shear	333.60	340.00	1.02
OA-2	shear	355.84	312.50	0.88
OA-3	shear	378.08	392.50	1.04
A-1	shear	467.04	442.50	0.95
A-2	shear	489.28	430.00	0.88
A-3	flexural	467.04	402.50	0.86
			Mean:	0.94

Table 2 Comparison of experimental and analytical ultimate loads (kN)

Experimental and analytical work	Method	*OA*-1	*A*-1
Bresler and Scordelis (1963)	experiment	333.60	467.02
Proposed method	semi-three-dimensional	340.0	442.5
Gonzalez-Vidosa, *et al.* (1991)	three-dimensional	300.0	450.0
Cedolin and Dei Poli†	two-dimensional	400.0	500.0
Bedard and Kotsovos†	two-dimensional	410.0	470.0
Balakrishnam and Murray†	two-dimensional	343.0	427.0

Note: † from Gonzalez-Vidosa, *et al.* (1991)

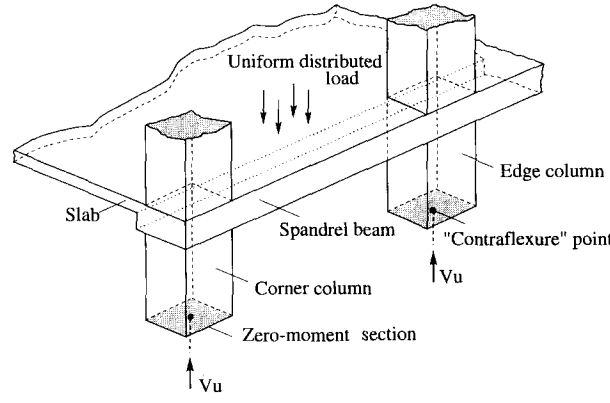

Fig. 9 Spandrel beam-column-slab connections.

methos as well as other finite element procedures as summarised by Gonzalez-Vidosa, *et al.* (1991).

The comparison indicates that the two-dimensional (plane stress) analyses, in general, overestimate the strength of the beams with or without web reinforcements. The proposed analysis and the method given by Gonzalez-Vidosa, *et al.*, on the other hand, yield better predictions. It appears that the proper modelling of the confinement caused by the closed ties may only be achieved by means of semi and full three-dimensional approaches.

5.2. Beam-column-slab connections in flat plate models

5.2.1. Structural details and modelling

As part of a long-term research program on the punching shear strength of concrete flat plates, a total of nine half-scale reinforced concrete models, each weighing about five tonnes, were constructed and tested to failure (Falamaki and Loo 1992). Fig. 9 shows a portion of a typical reinforced concrete flat plate structure with spandrel beams. Note that for a spandrel beam-column-slab connection, the punching shear strength, V_u, is defined as the net ultimate reaction at the column contraflexural point. The plan dimensions of the models and a typical cross section of spandrel beam-column-slab connection are shown in Figs. 10(a) and (b), respectively. Seven models having different spandrel beam depths, designated as *W*1 to *W*4 and *M*2 to *M*4, are investigated herein. The material properties and reinforcement details of the models

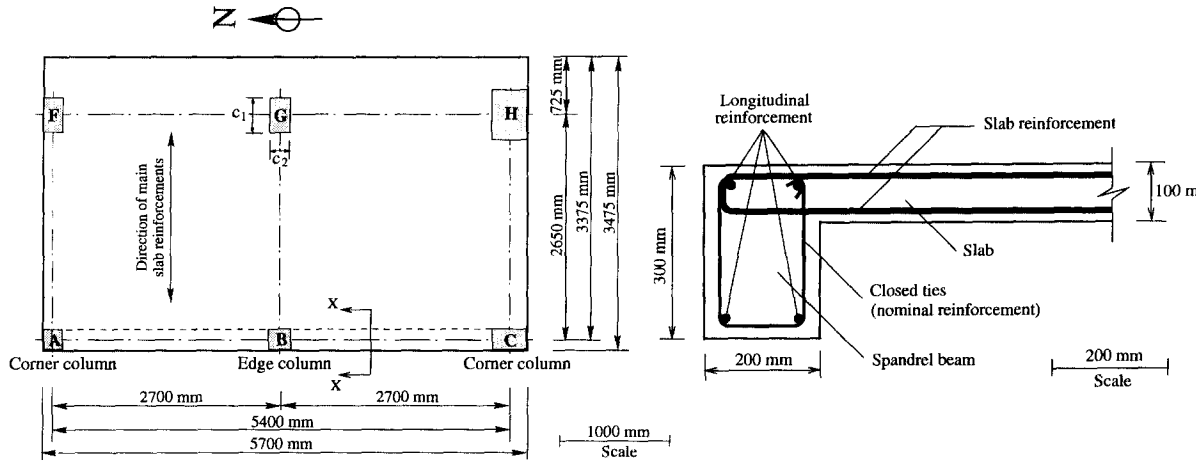

(a) Plan view (b) Section *x-x*

Fig. 10 Flat plate model with typical spandrel beam section details.

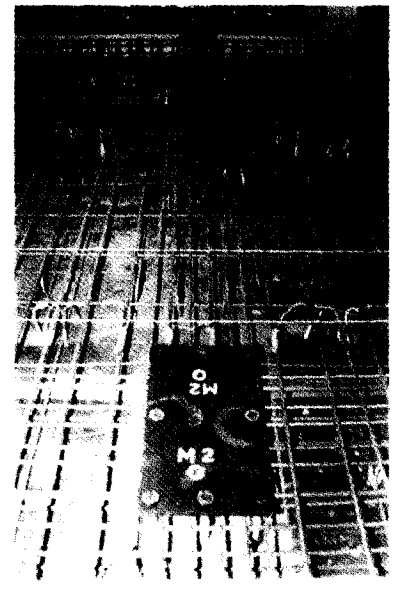

Fig. 11 Flexural reinforcement mesh in Model *M2*.

are based on those published by Falamaki and Loo (1992).

Each of the models had two layers of flexural reinforcement mesh near the top and bottom of the slab. A portion of the reinforcement mesh in a typical model (*M2*) is shown in Fig. 11. In addition, top reinforcing bars were added at column positions and bottom bars, at mid-span of the critical slab strips. They were provided to resist the large negative and positive bending moments at the respective positions. The longitudinal and transverse reinforcements of a typical spandrel beam are shown in Fig. 12.

To effectively model the reinforcement and construction details, a relatively fine mesh is required. For example, for Model *M2*, where a line load was applied and additional top and

Fig. 12 Longitudinal and transverse reinforcements in spandrel beam.

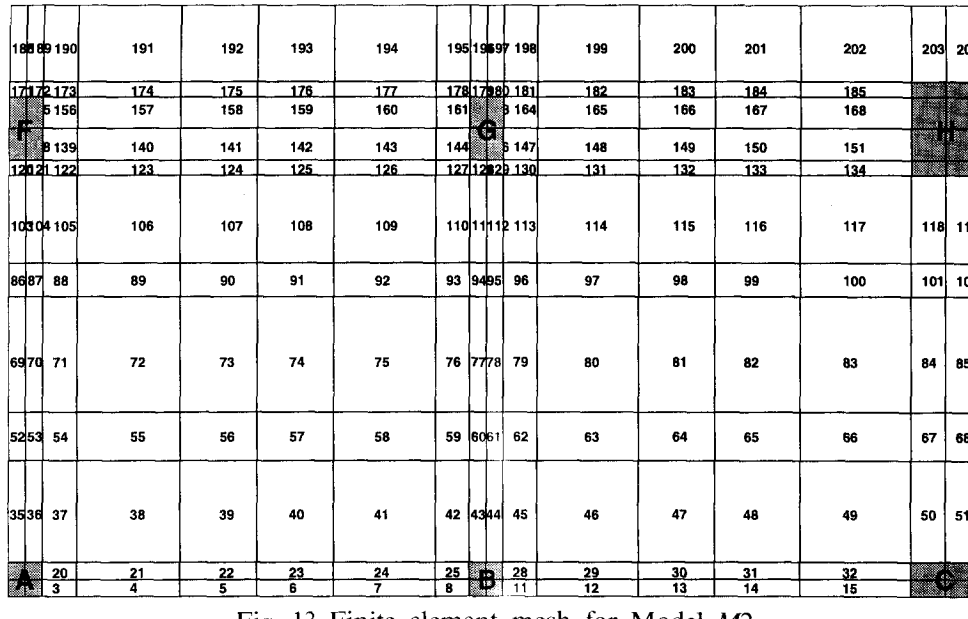

Fig. 13 Finite element mesh for Model *M2*.

bottom reinforcing bars were provided throughout the slab, a 17×12 mesh is used (see Fig. 13). Each element is subdivided into eight concrete layers of different thicknesses. The top and bottom reinforcement meshes are simulated by four steel layers. For other test models, a 14×12 mesh is adopted (Guan 1996).

5.2.2. Punching shear strength and collapse load

The predicted punching shear strength results (V_u) for the seven models with spandrel beams

Table 3 Comparison of punching shear strength V_u

Connection	Column type*	Experiment V_u (kN)	Proposed method	
			Predicted V_u (kN)	Predicted / Measured
W1-A	C	50.15	58.58	1.17
W2-A	C	48.08	52.88	1.10
W3-A	C	43.38	46.30	1.07
W4-A	C	47.07	52.14	1.11
W1-B	E	117.63	116.21	0.99
W2-B	E	120.36	104.79	0.87
W3-B	E	93.57	96.47	1.03
W2-C	C	45.17	46.70	1.03
W3-C	C	44.33	48.65	1.10
W4-C	C	46.32	50.79	1.10
M2-A	C	53.90	56.21	1.04
M3-A	C	25.70	34.10	1.33
M4-A	C	58.97	65.79	1.12
M2-B	E	123.22	115.43	0.94
M3-B	E	76.50	68.37	0.89
M4-B	E	130.24	149.69	1.15
M3-C	C	24.30	29.75	1.22
M4-C	C	60.09	74.50	1.24
			Mean:	1.08

Note: *C-corner column; E-edge column

Table 4 Comparison of collapse loads

Model	Experiment (kPa)	Proposed method	
		Predicted (kPa)	Predicted / Measured
W1	30.63	29.50	0.96
W2	28.91	30.00	1.04
W3	24.69	23.60	0.96
W4	28.95	25.75	0.89
M2	32.70†	37.50†	1.15
M3	17.84	15.60	0.87
M4	33.85	37.00	1.09
		Mean:	0.99

Note: †Line load in kN/m

are presented in Table 3. Also included in the table are the measured V_u as well as the ratios of the predicted and measured values. It can be seen that the proposed method is able to predict, with good accuracy, the punching shear strength results. The mean ratio of the predicted and measured V_u is 1.08 which is considered a satisfactory correlation.

Summarised in Table 4 is the comparison of the experimental and predicted collapse loads. The measured collapse loads are accurately predicted by the proposed method, with a mean ratio of 0.99 for the seven models.

5.2.3. Load-deflection responses

In Fig. 14, both the experimental and the predicted load-deflection results are presented for

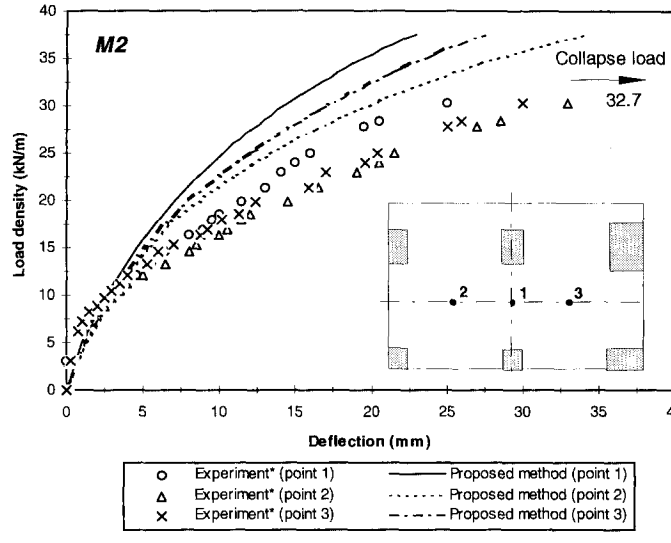

(* Falamaki and Loo, 1992)

Fig. 14 Comparison of load-deflection responses for Model *M2*.

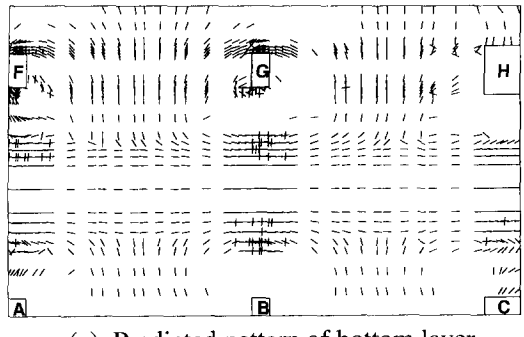

(a) Predicted pattern of bottom layer

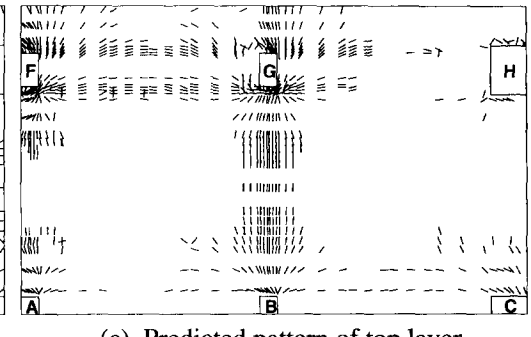

(c) Predicted pattern of top layer

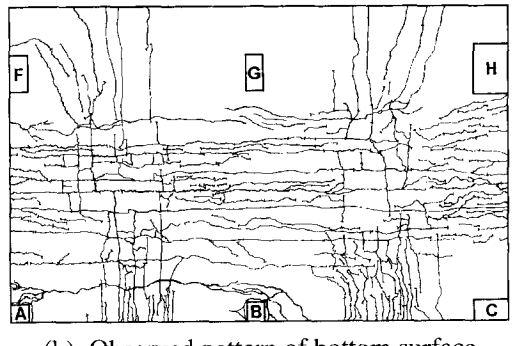

(b) Observed pattern of bottom surface

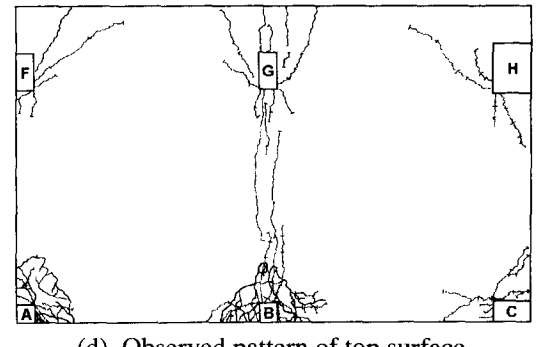

(d) Observed pattern of top surface

Fig. 15 Crack patterns for Model *M2*.

a typical model (*M*2). The proposed procedure is able to predict the actual load-deflection response reasonably well except that the predicted curves appear to be stiffer after cracking occurs. This discrepancy is mainly due to the relatively coarse (but effective and economical) mesh selected for modelling the real structure. The use of a finer but of course more expensive mesh will improve the correlation. The assumption of rigid support conditions in the analysis also contributes to the discrepancy. However, despite the discrepancies, the trends of the load-deflection behaviour are correctly predicted.

5.2.4. Crack patterns

The comparisons of the analytical and observed crack patterns at bottom and top surfaces of Model *M*2 are shown in Fig. 15. The crack directions predicted by the proposed method are consistent with the observations. Note however that analytically there are more cracks around the column regions at the bottom surface. In the proposed procedure, which is not unlike other similar nonlinear analyses, cracking can occur at any Gauss point once the concrete tensile strength has been reached. This means that any number of Gauss integration points can crack simultaneously. This unfortunately results in more cracks than reality where cracks tend to open relatively slowly and at fewer locations (Cope 1986). Further, physical cracks are only visible after a relatively large strain has been exceeded.

6. Conclusions

A nonlinear layered finite element method for cracking and failure analysis of reinforced concrete beams and the spandrel beam-column-slab connections of flat plate is presented. Both material and geometric nonlinearities are taken into consideration. Proper material models are established for concrete in tension and compression as well as for steel reinforcement. The spandrel beam and transverse reinforcement are also successfully modelled.

Comparisons with published test results are made for a series of simply supported beams and beam-column-slab connections. Analytical results obtained are in good agreement with the experimental observations in terms of load-deflection response, ultimate load as well as crack patterns. This confirms the capabilities and accuracy of the proposed method in analysing both flexural and shear failures as well as simulating transverse reinforcements.

The proposed layered procedure is capable of providing a simple and effective means of analysing the nonlinear behaviour and cracking of reinforced concrete beam-column-slab connections in flat plates. It is equally applicable to other similar three-dimensional problems.

Acknowledgements

The authors are grateful for the financial support granted by Griffith University, which also provided full access to the Queensland Parallel Supercomputing Facility located on Griffith's Nathan campus.

References

Bresler, B. and Scordelis, A.C. (1963), "Shear strength of reinforced concrete beams", *Journal of ACI,*

Proceedings, **60**(1), 51-72.

Cook, R.D., Malkus, D.S. and Plesha, M.E. (1989), *Concepts and Applications of Finite Element Analysis,* John Wiley & Sons, 630.

Cope, R.J. (1986), "Non-linear analysis of reinforced concrete slabs", *Computational Modeling of Reinforced Concrete Structures*, Hinton, E. and Owen, D.R.J. ed., 3-43.

Falamaki, M. and Loo, Y.C. (1992), "Punching shear tests of half-scale reinforced concrete flat plate models with spandrel beams", *ACI Structural Journal,* **89**(3), 263-271.

Guan, H. (1996), "Cracking and punching shear failure analysis of reinforced concrete flat plates by layered finite element method", PhD Thesis, Griffith University, Australia.

Guan, H. and Loo, Y.C. (1994), "Layered finite element method of failure analysis of reinforced concrete flat plates", *Proceedings of International Conference on Computational Methods in Structural and Geotechnical Engineering*, Hong Kong, 984-989.

Guan, H. and Loo, Y.C. (1996), "Numerical analysis and computer visualization of punching shear failure of reinforced concrete flat plates: Part I methodology", *Proceedings of The Third Asian-Pacific Conference on Computational Mechanics,* Seoul, Korea, 259-264.

Gonzalez-Vidosa, F., Kotsovos, M.D. and Pavlovic, M.N. (1991), "Three-dimensional non-linear finite-element model for structural concrete. Part 1: main features and objectivity study and Part 2: generality study", *Proceeding of Institution of Civil Engineers,* Part 2, **91**, 517-544 and 545-560.

Harmon, T.G. and Ni, Z. (1989), "Shear strength of reinforced concrete plates and shells determined by finite element analysis using layered elements", *Journal of Structural Engineering, ASCE,* **115**(5), 1141-1157.

Loo, Y.C. (1990), *Reinforced Concrete Analysis and Design,* University of Wollongong Press, New South Wales, 312.

Owen, D.R.J. and Figueiras, J.A. (1984), "Ultimate load analysis of reinforced concrete plates and shells including geometric nonlinear effects", *Finite Element Software for Plates and Shells,* Hinton, E. and Owen, D.R.J. ed., 327-388.